

## A Proton Nuclear Magnetic Resonance Assignment and Secondary Structure Determination of Recombinant Human Thioredoxin<sup>†</sup>

Julie D. Forman-Kay,<sup>‡,§</sup> G. Marius Clore,<sup>\*,†</sup> Paul C. Driscoll,<sup>†</sup> Paul Wingfield,<sup>||</sup> Frederic M. Richards,<sup>§</sup> and Angela M. Gronenborn<sup>\*,†</sup>

Laboratory of Chemical Physics, Building 2, National Institute of Diabetes and Digestive and Kidney Diseases, National Institutes of Health, Bethesda, Maryland 20892, Department of Molecular Biophysics and Biochemistry, Yale University, New Haven, Connecticut 06511, and Glaxo Institute for Molecular Biology S.A., 1211 Geneva 24, Switzerland

Received March 9, 1989; Revised Manuscript Received May 16, 1989

**ABSTRACT:** Two-dimensional <sup>1</sup>H NMR spectroscopy has been applied to a structural analysis of the reduced form of a recombinant human thioredoxin, a ubiquitous dithiol oxidoreductase recently isolated from an immunocompetent lymphoblastoid cell line. The sequential assignment of the spectrum, including all proline residues, has been accomplished by using experiments to demonstrate through-bond and through-space connectivities. The secondary structure has been determined by a qualitative interpretation of nuclear Overhauser effects, NH exchange data, and <sup>3</sup>J<sub>H<sub>N</sub>α coupling constants. The secondary structure was found to be similar to that of the X-ray structure of *Escherichia coli* thioredoxin, consisting of a mixed five-stranded β-sheet surrounded by four α-helices. The assignment and structural characterization of human thioredoxin was facilitated by the increased resolution and sensitivity afforded by a magnetic field strength of 600 MHz and required the use of two temperatures and two pH conditions to resolve ambiguities caused by a duplication of resonances. This duplication, extending from Phe-41 to Val-59, and including Lys-3-Ile-5, Val-24, Val-25, Asn-39, and Ile-101-Glu-103, appears to be due to heterogeneity arising from the presence or absence of the N-terminal methionine.</sub>

**H**uman thioredoxin is the most recently isolated of a group of ubiquitous proteins whose primary function is dithiol-disulfide oxidation and reduction (Wollman et al., 1988). A number of other thioredoxins have been identified from bacteria, bacteriophages, plants, and mammals, including those from *Escherichia coli* (Holmgren, 1985) and T4 bacteriophage (Söderberg et al., 1978) whose crystal structures have been determined. *E. coli*<sup>1</sup> thioredoxin, in particular, and its reconstitution systems have become models for protein folding studies (Reutimann et al., 1983; Thomas et al., 1986), and nuclear magnetic resonance (NMR) investigations of the solution structure of both the oxidized and reduced forms of the enzyme are in progress (LeMaster & Richards, 1988; Dyson et al., 1988). The *E. coli* protein, having 108 amino acids, is composed of a mixed five-stranded β-sheet surrounded by four α-helices and is divided into two supersecondary structural units. The first unit has a βαβαβ structure and contains the active-site disulfide which forms a 14-membered ring protruding from the surface of the protein. The second region is composed of a βαα unit and is connected to the first by a short α-helix and an irregular loop, as well as by hydrogen bonds between the β-strands of the two subdomains (Eklund et al., 1984). Human thioredoxin has 105 amino acids and is less than 25% homologous in its sequence to the *E. coli* protein, with exact homology only in the active-site region (Wollman et al., 1988). The homology is 30% for the N-terminal region of the molecule and only 18% for the rest of

the protein. Because of the potential for discovering a different folding pattern in the C-terminal portion of the molecule, a structural determination of human thioredoxin has been undertaken.

By use of two-dimensional <sup>1</sup>H NMR techniques to identify through-bond and through-space connections between the protons of the molecule (Wüthrich, 1986; Clore & Gronenborn, 1987), the spectrum of reduced human thioredoxin was assigned. The secondary structure was determined on the basis of a qualitative analysis of the NOE patterns, NH exchange data, and coupling constant information. The secondary structure of human thioredoxin is very similar to that of *E. coli*, in both subdomains of the protein, and thus no new C-terminal structural motif was found. However, an interesting characteristic of the protein system was noted. The <sup>1</sup>H NMR spectrum revealed a duplication of peaks corresponding primarily to amino acids<sup>2</sup> Phe-41-Val-59, and including

<sup>1</sup> Abbreviations: NMR, nuclear magnetic resonance; NOE, nuclear Overhauser effect; NOESY, two-dimensional NOE spectroscopy; COSY, homonuclear two-dimensional correlated spectroscopy; DQF-COSY, double quantum filtered correlated spectroscopy; PE-COSY, primitive exclusive correlated spectroscopy; HOHAHA, two-dimensional homonuclear Hartmann-Hahn spectroscopy; FID, free induction decay; DTT, dithiothreitol; *E. coli*, *Escherichia coli*.

<sup>2</sup> In the sequence numbering convention used in Wollmann et al. (1988), the recombinant human thioredoxin is numbered with valine-1 and the initiating methionine is disregarded. Although the *E. coli* bacteria in which the protein is expressed have the capacity to remove initiating methionines, with extremely overexpressed proteins, the system is taxed and the processing becomes inefficient. Gas-phase amino acid sequencing of the recombinant human thioredoxin indicated either 30% or 80% retention of the initiating methionine depending on the growth conditions. Because of the presence of this N-terminal methionine, as well as the coincidence that the active site and other conserved N-terminal sequences of *E. coli* and human thioredoxins line up if the methionine is counted, the convention of numbering the initiating methionine Met-1 and the following valine Val-2 has been adopted in this work.

<sup>†</sup> This work was supported by the Intramural AIDS Targeted Antiviral Program of the Office of the Director, NIH (G.M.C. and A.M.G.). J.D.F. acknowledges a graduate fellowship from the Molecular Biophysics and Biochemistry Department of Yale University and additional support from the National Institute of General Medical Sciences (GM-22778, F.M.R.).

<sup>‡</sup> National Institutes of Health.

<sup>§</sup> Yale University.

<sup>||</sup> Glaxo Institute for Molecular Biology S.A.

Lys-3-Ile-5, Val-24, Val-25, Asn-39, and Ile-101-Glu-103, which appears to be due to heterogeneity arising from the presence or absence of the N-terminal methionine.

#### EXPERIMENTAL PROCEDURES

**Purification of Recombinant Human Thioredoxin.** Human thioredoxin was expressed and purified from *E. coli* strain W3110cI containing a temperature-sensitive repressor and a plasmid bearing the human thioredoxin gene under control of the  $\lambda P_1$  promoter and the phage Mu *ner* gene ribosome binding site, as described by Wollman et al. (1988). The *E. coli* strain was grown under two sets of conditions; in the first, full medium was employed, while in the second, minimal medium was used. Expression of the protein was induced at 42 °C. Cells were lysed in a French press and centrifuged, and the resulting supernatant containing the human thioredoxin was purified by anion and cation ion-exchange chromatography using DEAE-Sephacrose and CM-Sephacrose with gradients from 0 to 0.5 M NaCl and from 0 to 0.25 M NaCl at pH values of 7.7 and 4.5, respectively, and a gel filtration column of AcA54 at pH 7.5. All column buffers contained 1 mM dithiothreitol (DTT).

N-Terminal amino acid sequence determination by automated Edman degradation was performed with a gas-phase sequencer (Applied Biosystems Model 470A). This revealed the presence of two species differing in the presence or absence of the N-terminal methionine. The ratio of the N-terminal amino acids of the two species was 80% N-Met/20% N-Val for the recombinant thioredoxin purified from *E. coli* grown in full medium and 30% N-Met/70% N-Val for the protein purified from *E. coli* grown in minimal medium.

**Sample Preparation.** Reduced human thioredoxin was prepared for NMR analysis by reducing 2 mM purified protein with excess DTT, dialyzing against 100–150 mM, pH 7.0 or 5.5, phosphate buffer containing 0.2 mM DTT, lyophilizing, and resolubilizing in argon-purged 90% H<sub>2</sub>O/10% D<sub>2</sub>O or 99.99% D<sub>2</sub>O. Samples were placed into argon-purged NMR tubes, sealed with airtight rubber septa, and blanketed with argon for 30 min. Solutions prepared in this way appear to be stable for at least 2 months, over a temperature range of 4–50 °C.

**NMR Spectroscopy: Data Collection and Processing.** <sup>1</sup>H NMR spectra were recorded on a Bruker AM600 600-MHz spectrometer and were processed on an ASPECT 3000 computer. HOHAHA (Braunschweiler & Ernst, 1983; Davis & Bax, 1985) and NOESY (Jeener et al., 1979; Macura et al., 1981) spectra were recorded at 25 and 40 °C in both H<sub>2</sub>O and D<sub>2</sub>O for samples at pH 7.0 and pH 5.5. For the NOESY experiments, mixing times of 100, 150, and 180 ms were used, and for the HOHAHA experiments, mixing times were 18, 36, and 46 ms. The HOHAHA experiment utilized a WALTZ17 mixing sequence (Bax, 1989) sandwiched between 1.5-ms trim pulses. DQF-COSY (Piantini et al., 1982; Rance et al., 1983) spectra were recorded at 40 °C and pH 7.0 in H<sub>2</sub>O and D<sub>2</sub>O. A PE-COSY (Mueller, 1987) experiment with a 35° mixing pulse was recorded, as described in Marion and Bax (1988a), at 40 °C and pH 5.5 in H<sub>2</sub>O. All of these 2D experiments were recorded in the pure phase absorption mode, using the time proportional incrementation method (Redfield & Kunz, 1975; Bodenhausen et al., 1980; Marion & Wüthrich, 1983). For NOESY and HOHAHA experiments, 1024 *t*<sub>1</sub> increments of 2K data points were collected and processed by appropriate zero-filling to give a digital resolution of 8 Hz/point in the *F*<sub>1</sub> dimension and 4 Hz/point in the *F*<sub>2</sub> dimension. For the DQF-COSY and PE-COSY experiments, 4K data points were collected for each *t*<sub>1</sub> increment, and the FIDs were

zero-filled to 1 Hz/point in *F*<sub>2</sub>. In the case of experiments carried out in H<sub>2</sub>O, water suppression was achieved either by coherent presaturation or by using sequences containing an on-resonance jump-return pulse sequence (Plateau & Guéron, 1982). For the HOHAHA spectra, a 90° “flip-back” pulse, a 100- $\mu$ s recovery delay, and the jump-return pulse sequence followed the WALTZ17 mixing sequence (Bax et al., 1987); for NOESY spectra, the jump-return pulse sequence replaced the last 90° pulse. Radiation damping was minimized by setting the preparation pulse 45° out of phase with the evolution and detection pulses (Driscoll et al., 1989). Spectra obtained with the jump-return water suppression sequence were processed by zeroing the first point and linearly base-line correcting each FID prior to Fourier transformation in the *F*<sub>2</sub> dimension and linearly base-line correcting the *F*<sub>2</sub> cross sections before Fourier transformation in *F*<sub>1</sub> (Driscoll et al., 1989). For all experiments, the receiver phase was optimized before the data were acquired to reduce base-line distortions (Marion & Bax, 1988b). This involved adjusting the relative receiver phase and the delay time between the detection pulse and the acquisition period so that the zero and first-order phase correction parameters for the *F*<sub>2</sub> Fourier transform were 90° and 180°, respectively.

#### RESULTS AND DISCUSSION

**Sample Oxidation.** Initially, the purified sample of human thioredoxin was dialyzed into phosphate buffer for NMR spectral data collection. Over the course of 2 weeks, however, the upfield methyl peaks showed significant broadening and shifts. SDS-polyacrylamide gel electrophoresis of the sample revealed dimerization of the protein, presumably due to intermolecular disulfide bond formation between any of the five cysteines of the protein, two of which are located in the active-site loop. Because the primary catalytic form of thioredoxin as a general protein disulfide reductase and specific hydrogen donor for such enzymes as ribonucleotide reductase is the reduced state and because of the aggregation problem, the reduced enzyme was chosen for structural studies. Sample preparation was modified to include the use of small quantities of DTT in the samples as well as argon-purged solvents and tubes to minimize the presence of oxygen and thus prevent oxidation of the cysteine side chains.

**Assignment.** The assignment of the <sup>1</sup>H NMR spectrum of reduced human thioredoxin was accomplished by using two-dimensional NMR techniques (Ernst et al., 1987) to identify through-bond and through-space connectivities (Wüthrich, 1986; Clore & Gronenborn, 1987). P.E-COSY and DQF-COSY spectra demonstrate direct through-bond scalar connectivities unambiguously, while HOHAHA spectra provide successively direct, single, and multiple relayed connectivities as the mixing time is increased. These intraresidue connectivities define the amino acid spin system to which particular groups of resonances belong. The NOESY spectra identify through-space (<5 Å) connectivities that give sequential interresidue information. Together, these methods provide a powerful method of “stepping through” the sequence of the protein and sequentially assigning the relevant proton resonances.

Analysis of the HOHAHA and NOESY spectra at pH 7.0 indicated the presence of more intraresidue NH-C $\alpha$ H cross-peaks than there are amino acids in the protein (Figure 1). This added spectral complexity necessitated the collection of another NMR data set at pH 5.5 to complete the assignment. Examples of these data can be seen in Figures 2–4. The stability of the folded protein that gives rise to slow amide exchange rates enabled observation of almost all amide protons



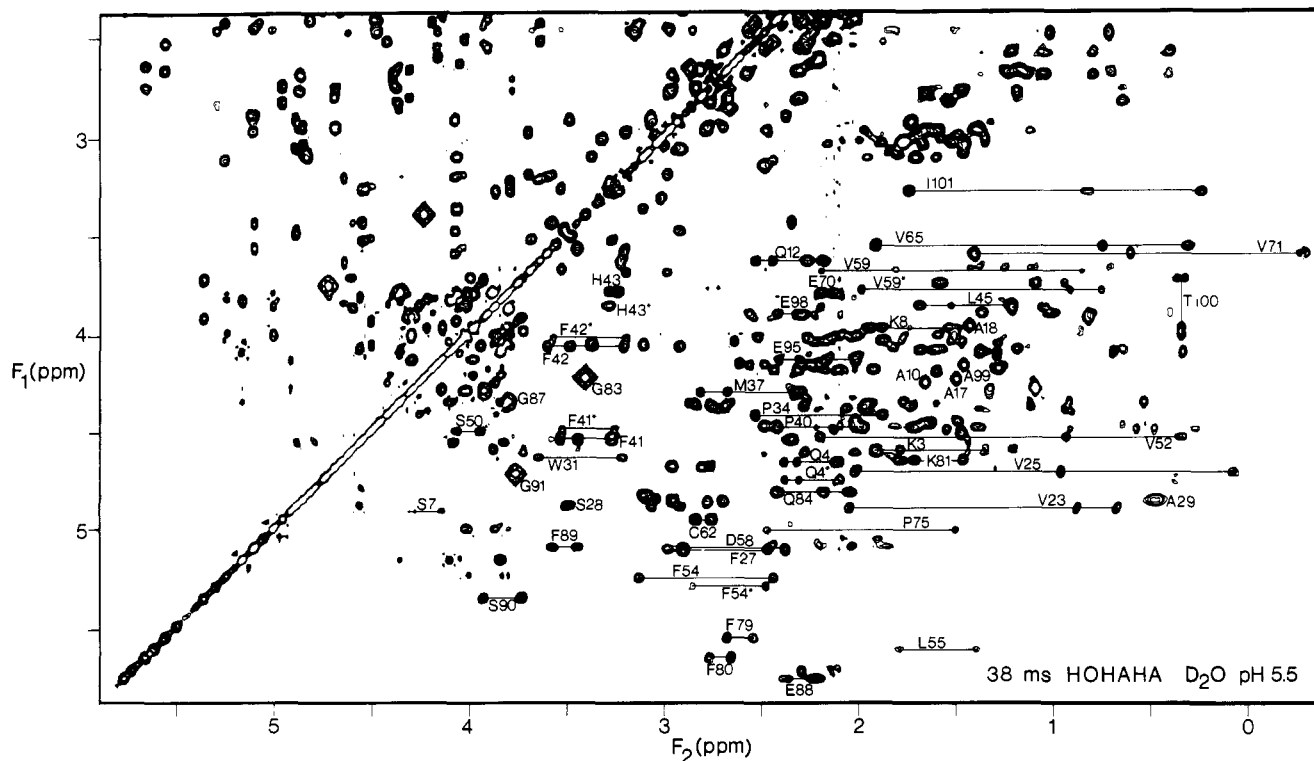


FIGURE 2: Aliphatic ( $F_2$  axis)-aliphatic ( $F_1$  axis) region of the 38-ms HOHAHA spectrum of the 80% N-Met/20% N-Val sample of recombinant human thioredoxin in  $D_2O$  at  $40^\circ C$  and pH 5.5. Some spin systems are indicated from residues in both forms. Residues of the minor N-terminal Val species are denoted with an asterisk.

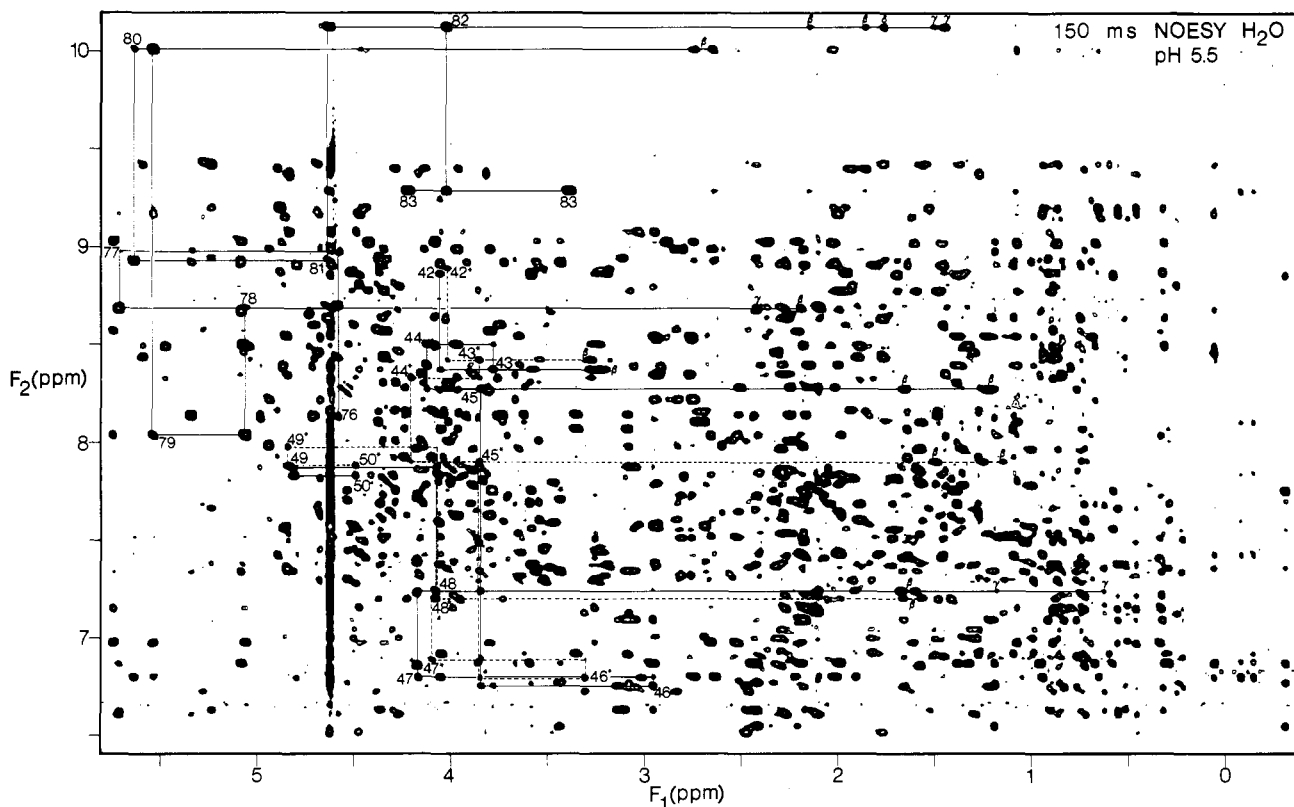


FIGURE 3: NH/aromatic ( $F_2$  axis)-aliphatic ( $F_1$  axis) region of the 150-ms NOESY spectrum of the 80% N-Met/20% N-Val sample of recombinant human thioredoxin in  $H_2O$  at  $40^\circ C$  and pH 5.5. Selected  $d_{\alpha N}(i, i + 1)$  connectivities are illustrated, including a region of the fourth  $\beta$ -strand ( $\beta_4$ ) from Thr-76 to Gly-83 and a region of the  $\alpha_2$  helix from Phe-42 to Ser-50. Those arising from residues in the dominant N-terminal Met species are indicated by continuous lines and those arising from residues in the minor N-terminal Val species by dashed lines. This latter group of resonances is denoted with an asterisk at the NH- $C_{\alpha}H$  cross-peak. Peaks are labeled at the NH( $i$ )- $C_{\alpha}H(i)$  intraresidue NOESY cross-peak.

under both pH conditions, as well as making possible extended experiments at  $40^\circ C$ , which significantly increased the spectral resolution by narrowing line widths. Clarification of the spectrum at pH 5.5 and  $40^\circ C$  indicated a duplication of

resonances, predominantly in the region from Phe-41 to Val-59, as well as that from Lys-3 to Ile-5, from Val-24 to Val-25, Asn-39, and from Ile-101 to Glu-103, with one set of peaks significantly weaker in intensity than the other. In

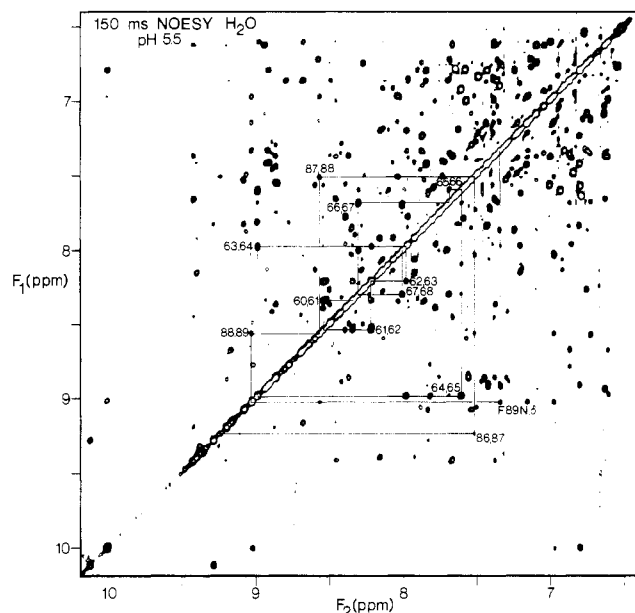


FIGURE 4: NH/aromatic ( $F_2$  axis)–NH/aromatic ( $F_1$  axis) region of the 150-ms NOESY spectrum of the 80% N-Met/20% N-Val sample of recombinant human thioredoxin in  $H_2O$  at 40 °C and pH 5.5. The sequence of  $d_{NN}(i, i + 1)$  NOE connectivities for residues Asp-60–Glu-68, located in  $\alpha_3$ , is indicated, as well as the sequence of connectivities for residues Val-86–Phe-89 of  $\beta_5$ , with the intraresidue Phe-89 NH– $C_\beta$ H NOE.

most cases the duplicate peak was close in chemical shift, but in some cases, the corresponding peaks were displaced by close to 0.4 ppm (cf. Leu-45 NH, Ser-46  $C_\alpha$ H, and Phe-54 NH).

N-Terminal amino acid sequencing indicated the presence of two species of recombinant human thioredoxin, differing in the presence or absence of the N-terminal methionine. The original sample on which most of the NMR work was carried out was purified from *E. coli* grown in full medium, and the ratio of the N-terminal amino acids of the two species was approximately 80% N-Met/20% N-Val. A later sample purified from *E. coli* grown in minimal medium contained approximately 30% N-Met/70% N-Val in the first position. Thus, the efficiency of removal of the translation-initiating methionine seems to be dependent upon the fermentation conditions used. The ratio of the intensities of the two sets of peaks observed in both samples is the same, within experimental error, to the ratio of the two species present in the sample. This strongly suggests that the duplication of the resonances arises directly from the sequence heterogeneity at the N-terminus.

As a result of the duplication found for resonances of approximately one-third of the amino acids in the sequence, the assignment of the spectrum was more challenging than might otherwise have been anticipated. Often, the NH shift was the most sensitive and the aliphatic protons were degenerate. Because of the general similarity in chemical shift, the resolution and sensitivity of the 600-MHz spectrometer was very helpful for the elucidation of the second set of peaks in the spectrum of recombinant human thioredoxin. In addition, the presence of two sets of peaks and two samples with inverted species populations proved useful for verifying assignments. Examples of HOHAHA and NOESY spectra from the 80% N-Met/20% N-Val sample are shown in Figures 1–4.

Table I lists the assignments of the  $^1H$  NMR spectrum of human thioredoxin. All residues of the molecule have been unambiguously assigned, except the N-terminal amino acids of the two species. In the case of the N-Met form, the Val-2 to Lys-3 sequential connectivity is readily identified. An ad-

ditional valine spin system lacking sequential NOE connections is tentatively assigned to the Val-2\* of the N-Val species ( $C_\alpha$ H, 3.81;  $C_\beta$ H, 1.98;  $C_\gamma$ H<sub>3</sub>, 0.91 and 0.75). The chemical shifts are reported to an accuracy of  $\pm 0.02$  ppm at 40 °C and pH 5.5. The chemical shifts of the duplicate peaks, where distinguishable, are given below those for the major peak. Note the differences in chemical shift between the assignments shown for each pair of duplicate resonances. Other residues showed signs of small differences in chemical shifts, but these were not resolvable. Throughout the table, the presentation of one chemical shift for the  $C_\beta$  or other side-chain protons does not imply degeneracy. It may be that the other proton has not been located or that the two protons overlap to a significant degree so that unambiguous determination of the center of each peak is difficult.

A summary of the sequential connectivities involving the NH,  $C_\alpha$ H, and  $C_\beta$ H protons, as well as the  $C_\beta$ H protons of proline residues, is shown in Figure 5. No significant differences in either the pattern or relative intensities of the NOEs could be observed for those residues whose resonances had different chemical shifts in the two species.

*Secondary Structure of Human Thioredoxin.* The presence of both  $\beta$ -sheet and  $\alpha$ -helical regions was immediately apparent from a qualitative interpretation of the data used in the sequential analysis. Extended strands were deduced from stretches of  $d_{\alpha N}(i, i + 1)$  connectivities with accompanying large values of the apparent  $^3J_{HN\alpha}$  coupling constants, while helical structures were evident from stretches of  $d_{NN}(i, i + 1)$ ,  $d_{NN}(i, i + 2)$ ,  $d_{\alpha N}(i, i + 2)$ ,  $d_{\alpha N}(i, i + 3)$ ,  $d_{\alpha\beta}(i, i + 3)$ , and  $d_{\alpha N}(i, i + 4)$  connectivities. The specific secondary structural elements of the protein were identified on the basis of a qualitative interpretation of short-range NOEs, long-range NOEs between adjacent  $\beta$ -strands, NH exchange data, and apparent  $^3J_{HN\alpha}$  coupling constants (Wüthrich et al., 1984). The summary of these data is presented in Figure 5. The suggested secondary structure is outlined above the sequence. NH exchange data refer to those amide protons that are protected from exchange with  $D_2O$  and are reported from a HOHAHA spectrum of a sample that had been lyophilized from  $H_2O$  and then freshly dissolved in  $D_2O$ . The  $^3J_{HN\alpha}$  coupling constants were measured from a PE-COSY spectrum and were found to fall into two classes, those less than 9 Hz and those greater than 9 Hz. These values have not been adjusted to remove the effects of the line width and therefore seem large (Neuhaus et al., 1985). The set larger than 9 Hz has been roughly interpreted as corresponding to  $\phi$  torsion angles that would be representative of an extended conformation (Bystrov, 1976; Pardi et al., 1984). This method of interpretation of the data shown in Figure 5 does not yield absolutely certain identification of the beginnings and ends of helices, since the pattern of NOEs in potential tight turns preceding or following a helix is very similar to that within the helix itself. A more exact determination of the extent of the helices will come out of the tertiary structure. The beginnings and ends of  $\beta$ -sheets, however, can be assigned using this method with a greater degree of confidence on the basis of the interstrand NOEs (see Figure 6).

By use of this qualitative pattern recognition approach, the secondary structure of human thioredoxin was found to be similar to that of *E. coli* thioredoxin, with a mixed five-stranded  $\beta$ -sheet and four  $\alpha$ -helices. The  $\beta$ -sheet structure is illustrated in Figure 6. It is composed of hydrogen-bonding networks between a triple-stranded antiparallel  $\beta$ -sheet and triple-stranded parallel  $\beta$ -sheet with a central strand common to both. The five strands conserve the same orientation and

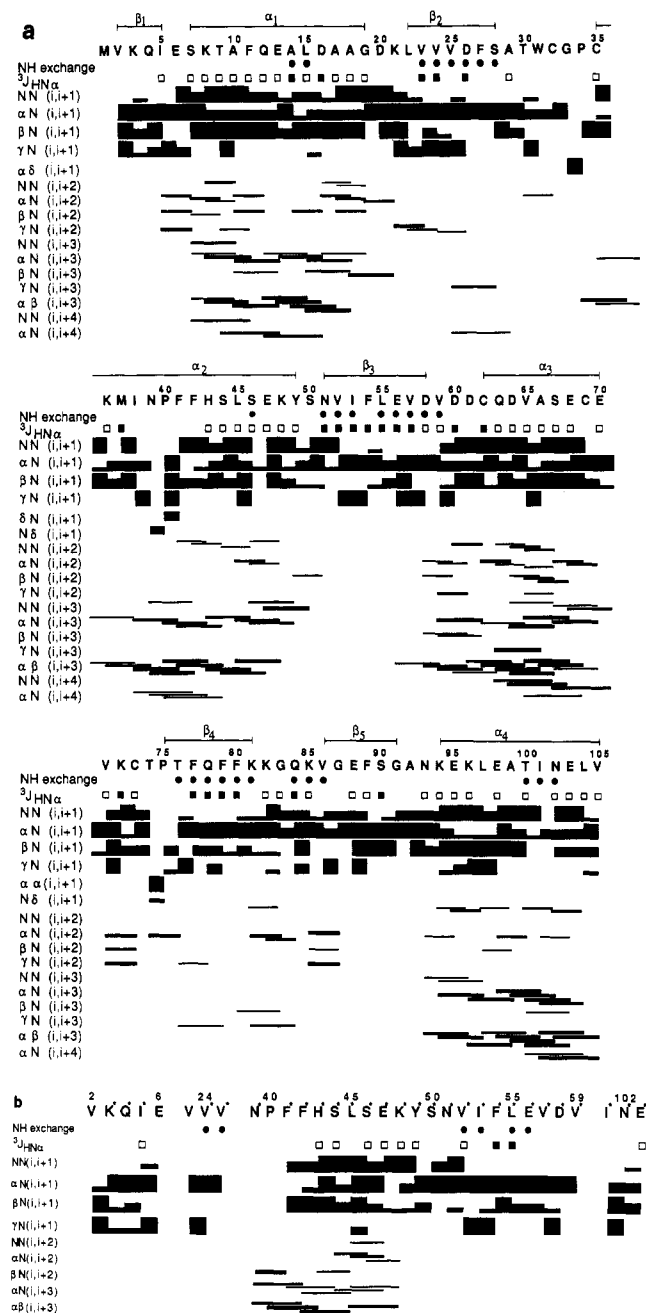


FIGURE 5: (a) Sequence of human thioredoxin and summary of the short-range NOEs for residues in the N-terminal Met species involving the NH, C<sub>α</sub>H, C<sub>β</sub>H, and C<sub>γ</sub>H protons, as well as the C<sub>δ</sub>H protons of proline residues, the slowly exchanging NH protons, and the apparent  $^3J_{\text{HN}\alpha}$  coupling constants, with the secondary structure deduced from them. (b) Summary of short-range NOEs for residues in the N-terminal Val species that have different chemical shifts from those in the N-terminal Met species, denoted by an asterisk, along with NH exchange and apparent  $^3J_{\text{HN}\alpha}$  data. The NOEs are classified as strong, medium, and weak, indicated by the thickness of the lines. Backbone amide NH protons that are still present after the protein is dissolved in D<sub>2</sub>O are indicated by solid circles, and apparent values of  $^3J_{\text{HN}\alpha} > 9$  Hz and  $^3J_{\text{HN}\alpha} < 9$  Hz are indicated by solid and open squares, respectively. Intensities were taken from the NOESY spectra at 40 °C and pH 5.5.

relation to each other as those in *E. coli* thioredoxin.  $\beta$ -Strand 5 may not be entirely regular, as suggested by the stretch of  $d_{\text{NN}}(i, i + 1)$  NOEs seen in that region, which would not be expected in an ideal extended strand. Helices are interspersed in the primary sequence between the  $\beta$ -strands and presumably lie on the surface of the protein, with the  $\beta$ -sheet at the core. Not all NH protons expected to be protected from exchange

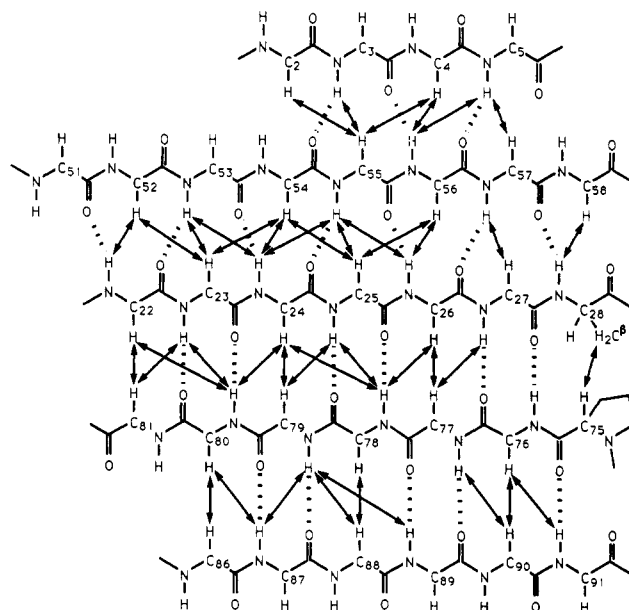


FIGURE 6: Schematic representation of the  $\beta$ -sheet of human thioredoxin deduced from a qualitative analysis of the NMR data. The observed interstrand NOE connectivities between backbone NH and C<sub>α</sub>H or C<sub>β</sub>H protons of the five strands are indicated by arrows, and hydrogen bonds suggested by NOE patterns and slowly exchanging amide protons are marked with dotted lines.

on the basis of these secondary structural elements are observed in D<sub>2</sub>O spectra. This is probably due to the pH of 5.5 at which the spectra were recorded, a point far from the minimum of the exchange curve for internal NH protons, which falls at approximately pH 3 (Wüthrich & Wagner, 1979). Table II presents a comparison of the secondary structural features of *E. coli* (Eklund et al., 1984; LeMaster & Richards, 1988) and human thioredoxins.

The far-UV circular dichroism spectrum (240–190 nm) of human thioredoxin was analyzed in 100 mM Tris-HCl at pH 7.5. The spectrum looked similar to that shown by Kelley and Stellwagon (1984) for the oxidized *E. coli* enzyme. Computer analysis of the CD spectrum indicated  $\alpha$ -helix and  $\beta$ -sheet contents of 49% and 35%, respectively, by the method of Chang et al. (1978). This result indicates substantial helix and sheet structure consistent with the NMR analysis, which has determined 43%  $\alpha$ -helix and 31%  $\beta$ -sheet.

As with the *E. coli* thioredoxin, the human protein contains a high percentage of regular secondary structure, approximately 75% (Holmgren, 1985), and the secondary structural elements within the two enzymes are similar, even though the overall amino acid homology is less than 25%. A notable exception is the third helix of *E. coli* thioredoxin, which is significantly shorter than that in the human enzyme, extending only for one turn, as compared to almost three turns. The one-turn helix of *E. coli* thioredoxin, from residue 59 to residue 63, is followed by a loose helical loop containing two prolines at positions 64 and 66. The human thioredoxin's  $\alpha$ -helix, extending from residue 63 to residue 70, may be preceded by a one-turn helical loop and contains a longer helix in place of the loose helical loop of *E. coli*. This is probably due to the absence of the two prolines. The five strands and other three helices line up rather well, allowing for a one- or two-residue shift in the alignment of the two sequences and the approximate determination of the beginnings and ends of these elements (see Table II).

In addition, the conformations of the proline peptide bonds are conserved between the two structures. Human thioredoxin has three prolines, at positions 34, 40, and 75, while *E. coli*

Table I: Proton Resonance Assignments of Human Thioredoxin at 40 °C and pH 5.5<sup>a</sup>

residue	chemical shift (ppm)			
	NH	C <sub>α</sub> H	C <sub>β</sub> H	other
M1	<i>b</i>	<i>b</i>	<i>b</i>	<i>b</i>
V2	8.63	4.36	1.77	C <sub>γ</sub> H 0.91, 0.53
K3	8.43	4.61	1.92, 1.78	C <sub>γ</sub> H 1.42, 1.35; C <sub>ε</sub> H 3.01
K3*	8.44	4.63	<i>c</i>	<i>c</i>
Q4	8.70	4.67	2.11	C <sub>γ</sub> H 2.39, 2.32; N <sub>ε</sub> H <sub>2</sub> 7.61, 6.93
Q4*	8.68	4.76	2.09	C <sub>γ</sub> H 2.38, 2.31
I5	8.63	4.38	2.28	C <sub>γm</sub> H 1.11
I5*	8.65	4.35	2.26	C <sub>γm</sub> H 1.12
E6	8.91	4.62	2.02	C <sub>γ</sub> H 2.35, 2.28
S7	7.42	4.92	4.29, 4.14	
K8	9.39	3.98	1.95, 1.88	C <sub>γ</sub> H 1.53, 1.49; C <sub>δ</sub> H 1.73, 1.69; C <sub>ε</sub> H 3.00
T9	8.15	4.06	2.21, 1.99	C <sub>γ</sub> H 1.28
A10	7.92	4.26	1.65	
F11	8.07	4.07	3.37, 3.11	C <sub>δ</sub> H 6.94; C <sub>ε</sub> H 7.02; C <sub>ζ</sub> H 6.63
Q12	8.14	3.64	2.26, 2.18	C <sub>γ</sub> H 2.53, 2.44; N <sub>ε</sub> H <sub>2</sub> 7.64, 6.78
E13	8.28	4.03	2.11, 2.02	C <sub>γ</sub> H 2.52, 2.26
A14	7.83	4.10	1.37	
L15	7.60	3.75	1.58, 1.09	C <sub>γ</sub> H 0.94; C <sub>δ</sub> H -0.13, -0.07
D16	8.10	4.39	2.76, 2.69	
A17	8.15	4.24	1.49	
A18	7.19	3.97	1.43	
G19	7.62	3.98, 3.81		
D20	8.99	4.69	2.81	
K21	7.81	4.36	1.96	C <sub>γ</sub> H 1.60; C <sub>δ</sub> H 1.70; C <sub>ε</sub> H 3.11
L22	8.78	4.45	2.02	C <sub>γ</sub> H 1.49; C <sub>δ</sub> H 1.09, 0.91
V23	9.02	4.90	2.04	C <sub>γ</sub> H 0.88, 0.67
V24	9.20	4.49	1.55	C <sub>γ</sub> H 0.57, 0.48
V24*	9.15	4.47	1.63	C <sub>γ</sub> H 0.64, 0.52
V25	9.16	4.70	2.02	C <sub>γ</sub> H 0.96, 0.07
V25*	9.18	4.72	<i>c</i>	<i>c</i>
D26	8.46	4.31	2.33	
F27	8.79	5.11	2.98, 2.47	C <sub>δ</sub> H 6.89; C <sub>ε</sub> H/C <sub>ζ</sub> H 7.36
S28	8.67	4.89	3.50	
A29	7.36	4.86	0.47	
T30	9.37	3.83	4.18	C <sub>γ</sub> H 1.27
W31	6.79	4.64	3.65, 3.22	C <sub>β3</sub> H 7.45; C <sub>β5</sub> H 7.17 C <sub>γ2</sub> H 7.23; C <sub>β2</sub> H 7.50 C <sub>β1</sub> H 7.31; N <sub>ε1</sub> H 11.21
C32	6.52	4.48	2.48, 1.81	
G33	<i>d</i>	4.30, 3.92		
P34		4.43	2.53, 1.87	C <sub>γ</sub> H 2.29, 2.10; C <sub>δ</sub> H 4.62, 3.72
C35	7.59	4.07	3.49, 2.92	
K36	7.79	4.01	2.09, 2.00	C <sub>γ</sub> H 1.59, 1.51; C <sub>δ</sub> H 1.76; C <sub>ε</sub> H 3.02
M37	7.83	4.31	2.30	C <sub>γ</sub> H 2.81, 2.67
I38	7.62	4.69	2.00	C <sub>γm</sub> H 1.29; C <sub>γ</sub> H 1.93, 1.84 C <sub>δ</sub> H 1.01
N39	7.68	4.39	2.06, 1.73	
N39*	7.64	4.34	2.02, 1.71	
P40		4.49	2.42, 2.02	C <sub>γ</sub> H 2.22, 2.09; C <sub>δ</sub> H 3.91, 3.82
F41	7.44	4.55	3.54, 3.27	C <sub>δ</sub> H 7.32; C <sub>ε</sub> H/C <sub>ζ</sub> H 7.56
F41*	7.46	4.51	3.53, 3.26	C <sub>δ</sub> H 7.29; C <sub>ε</sub> H/C <sub>ζ</sub> H 7.53
F42	8.86	4.07	3.60, 3.21	C <sub>δ</sub> H 7.40; C <sub>ε</sub> H/C <sub>ζ</sub> H 7.69
F42*	8.89	4.03	3.57, 3.19	C <sub>δ</sub> H 7.38; C <sub>ε</sub> H/C <sub>ζ</sub> H 7.71
H43	8.37	3.80	3.28, 3.23	C <sub>β2</sub> H 7.39; C <sub>ε1</sub> H 8.10
H43*	8.42	3.87	3.28	C <sub>β2</sub> H 7.31; C <sub>ε1</sub> H 8.16
S44	8.50	4.14	3.99	
S44*	8.33	4.22	3.98	
L45	8.27	3.87	1.68, 1.21	
L45*	7.90	3.87	1.52, 1.17	
S46	6.75	2.98	2.48	
S46*	6.79	3.32	3.02	
E47	6.79	4.18	2.11, 1.92	C <sub>γ</sub> H 2.23, 2.03
E47*	6.88	4.11	2.00	C <sub>γ</sub> H 2.34
K48	7.23	4.09	1.68, 1.61	C <sub>γ</sub> H 1.19, 0.64; C <sub>δ</sub> H 1.54, 1.46 C <sub>ε</sub> H 2.93, 2.78
K48*	7.20	4.09	1.67, 1.57	<i>c</i>
Y49	7.88	4.85	3.10, 3.06	C <sub>δ</sub> H 7.37; C <sub>ε</sub> H 6.93
Y49*	7.97	4.86	3.10	C <sub>δ</sub> H 7.40; C <sub>ε</sub> H 6.89
S50	7.83	4.50	4.07, 3.94	
S50*	7.88	4.50	<i>c</i>	
N51	9.07	4.85	3.05, 2.98	N <sub>δ</sub> H <sub>2</sub> 7.58, 6.79
N51*	9.05	4.85	<i>c</i>	<i>c</i>
V52	7.53	4.58	2.19	C <sub>γ</sub> H 0.93, 0.34
V52*	7.49	4.48	2.12	C <sub>γ</sub> H 0.91, 0.24
I53	8.86	4.38	1.96	C <sub>γm</sub> H 0.93
I53*	8.80	4.40	1.94	C <sub>γm</sub> H 0.90
F54	8.94	5.24	3.13, 2.44	C <sub>δ</sub> H 6.65; C <sub>ε</sub> H 7.12; C <sub>ζ</sub> H 6.77
F54*	8.57	5.29	2.85, 2.48	C <sub>δ</sub> H 6.74; C <sub>ε</sub> H 7.15; C <sub>ζ</sub> H 6.80
L55	9.41	5.60	1.78, 1.38	C <sub>γ</sub> H 1.57; C <sub>δ</sub> H 0.86, 0.61

Table I (Continued)

residue	chemical shift (ppm)			
	NH	C <sub>α</sub> H	C <sub>β</sub> H	other
L55*	9.42	5.49	1.75, 1.35	C <sub>γ</sub> H 1.54; C <sub>δ</sub> H 0.87, 0.62
E56	8.49	5.09	1.85	C <sub>γ</sub> H 2.20, 2.04
E56*	8.48	5.05	1.90	C <sub>γ</sub> H 2.21, 2.07
V57	8.49	4.10	1.33	C <sub>γ</sub> H 0.69, 0.33
V57*	8.41	4.31	1.32	c
D58 <sup>a</sup>	9.02	5.10	2.90, 2.38	
V59	8.93	3.68	2.18	C <sub>γ</sub> H 0.98, 0.86
V59*	f	c	2.19	C <sub>γ</sub> H 0.98, 0.85
D60	8.34	4.86	2.95, 2.78	
D61	8.54	4.69	2.97, 2.78	
C62	8.21	4.94	2.84, 2.76	
Q63	7.98	4.16	2.19	C <sub>γ</sub> H 2.61
D64	8.99	4.36	2.86, 2.67	
V65	7.60	3.56	1.91	C <sub>γ</sub> H 0.74, 0.30
A66	7.69	3.61	1.40	
S67	8.30	4.30	4.02	
E68	8.00	4.15	2.27, 2.20	C <sub>γ</sub> H 2.56, 2.48
C69	7.70	4.54	3.45, 2.33	
E70	7.75	3.80	2.12	C <sub>γ</sub> H 2.19
V71	7.75	3.59	1.40	C <sub>γ</sub> H 0.60, -0.29
K72	8.86	4.48	1.98, 1.71	C <sub>γ</sub> H 1.38; C <sub>δ</sub> H 2.97
C73	7.55	4.87	3.06, 2.92	
T74	8.38	4.74	3.92	C <sub>γ</sub> H 0.81
P75		5.01	2.47, 1.50	C <sub>γ</sub> H 1.82; C <sub>δ</sub> H 3.69, 3.53
T76	8.13	4.60	3.88	C <sub>γ</sub> H 1.20
F77	8.98	5.74	2.29, 2.18	C <sub>δ</sub> H 6.65; C <sub>γ</sub> H 7.06; C <sub>ε</sub> H 6.96
Q78	8.69	5.07	2.21, 1.99	C <sub>γ</sub> H 2.43
F79	8.03	5.56	2.68, 2.54	C <sub>δ</sub> H 7.00; C <sub>γ</sub> H 7.18; C <sub>ε</sub> H 7.25
F80	10.01	5.66	2.77, 2.66	C <sub>δ</sub> H 6.82; C <sub>γ</sub> H 7.45; C <sub>ε</sub> H 7.87
K81	8.93	4.66	1.79, 1.71	C <sub>γ</sub> H 1.46; C <sub>δ</sub> H 1.81; C <sub>ε</sub> H 3.09
K82	10.12	4.04	2.16, 1.88	C <sub>γ</sub> H 1.52, 1.46; C <sub>δ</sub> H 1.78 C <sub>ε</sub> H 3.04
G83	9.28	4.23, 3.41		
Q84	7.83	4.82	2.18, 2.05	C <sub>γ</sub> H 2.42
K85	8.90	4.07	1.82	C <sub>γ</sub> H 1.13; C <sub>δ</sub> H 2.97
V86	9.24	4.62	2.48	C <sub>γ</sub> H 1.01, 0.71
G87	7.51	4.36, 3.81		
E88	8.57	5.77	2.23, 2.19	C <sub>γ</sub> H 2.37
F89	9.03	5.10	3.58, 3.45	C <sub>δ</sub> H 7.36; C <sub>γ</sub> H 7.42; C <sub>ε</sub> H 6.87
S90	8.92	5.37	3.93, 3.74	
G91	8.13	4.72, 3.77		
A92	8.60	4.51	1.47	
N93	7.57	4.86	2.96, 2.70	
K94	8.54	3.67	1.42, 1.36	C <sub>γ</sub> H 0.72; C <sub>δ</sub> H 1.24, 1.10; C <sub>ε</sub> H 2.68
E95	8.39	4.13	2.15, 2.00	C <sub>γ</sub> H 2.40, 2.29
K96	7.78	3.89	1.36, 1.01	C <sub>γ</sub> H 0.78, 0.39; C <sub>δ</sub> H 1.21, 1.04 C <sub>ε</sub> H 2.69, 2.58
L97	7.96	4.20	2.31	C <sub>γ</sub> H 1.60; C <sub>δ</sub> H 0.88, 0.74
E98	7.85	3.89	2.31, 2.28	C <sub>γ</sub> H 2.41
A99	8.35	4.16	1.46	
T100	8.03	3.72	4.00	C <sub>γ</sub> H 0.35
I101	7.45	3.28	1.74	C <sub>γm</sub> H 0.23
I101*	7.50	3.28	c	c
N102	7.51	4.36	2.82, 2.77	
N102*	7.55	4.38	2.83, 2.78	
E103	7.73	4.19	2.18, 2.09	C <sub>γ</sub> H 2.43
E103*	7.71	c	c	c
L104	7.41	4.46	1.48	C <sub>γ</sub> H 1.63; C <sub>δ</sub> H 0.76, 0.37
V105	7.49	3.88	2.19	C <sub>γ</sub> H 1.06, 1.04

<sup>a</sup>Residues with chemical shifts for the N-terminal Val species that are distinguishable from those of the N-terminal Met species are indicated by an asterisk. Chemical shifts are expressed relative to 4,4-dimethyl-4-silapentane-1-sulfonate and measured with respect to the water resonance that has a chemical shift of 4.62 ppm at 40 °C. <sup>b</sup>Resonance not detected. <sup>c</sup>The N-terminal Val form resonance is degenerate with the N-terminal Met form resonance or virtually indistinguishable. <sup>d</sup>Gly-33 NH resonance not detected at pH 5.5 and 40 °C; at pH 7.0 and 25 °C the NH resonates at 9.22 ppm. <sup>e</sup>At 25 °C the resonances of Asp-58 for the N-terminal Val form are clearly distinguishable, with the NH at 9.04 ppm and the C<sub>α</sub>H at 5.13 ppm. <sup>f</sup>The Val-59\* NH resonance of the N-Val form is not detected at 40 °C, but at 25 °C the NH resonates at 8.96 ppm.

thioredoxin contains five, at positions 34, 40, 64, 68, and 76. Three of these proline sites are conserved between the sequences of the bacterial and human forms of the enzyme. In the crystal structure of *E. coli* thioredoxin, all proline peptide bonds are in the trans conformation except Pro-76, which is cis (Eklund et al., 1984). In the case of a trans peptide bond, the C<sub>α</sub>H of the preceding residue is in close proximity to at least one of the C<sub>β</sub>H protons of the proline, while in the cis conformation, the C<sub>α</sub>H of the preceding residue is close in

space to the C<sub>α</sub>H of the proline. In the human protein, Pro-34 is in the trans conformation, while Pro-75 exhibits a cis bond, as evidenced by diagnostic NOEs between the C<sub>α</sub>H of Gly-33 and the C<sub>β</sub>H of Pro-34 and between the C<sub>α</sub>H of Thr-74 and the C<sub>α</sub>H of Pro-75, respectively. In the case of Pro-40, the peak diagnostic of a trans conformer could not be unambiguously identified due to the presence of an intense Gly-87 C<sub>α</sub>H-C<sub>α</sub>H cross-peak at the position of the probable Asn-39 C<sub>α</sub>H-Pro-40 C<sub>β</sub>H cross-peak. A small NOE partially over-

Table II: Comparison of the Secondary Structure of *E. coli* and Human Thioredoxins

secondary structural element	<i>E. coli</i> thioredoxin residue positions <sup>a</sup>	human thioredoxin residue positions
$\beta$ -strand 1	D2-T8	V2-I5
$\alpha$ -helix 1	S11-K18	S7-G19
$\beta$ -strand 2	A22-A29	L22-S28
$\alpha$ -helix 2	C35-Y49	C35-Y49
$\beta$ -strand 3	L53-L58	N51-D58
$\alpha$ -helix 3	N59-N63	C62-E70
$\beta$ -strand 4	T77-F81	P75-K81
$\beta$ -strand 5	A88-V91	V86-G91
$\alpha$ -helix 4	S95-L107	K94-V105

<sup>a</sup>The secondary structure of *E. coli* thioredoxin presented is taken from both the X-ray (Eklund et al., 1984) and NMR (LeMaster & Richards, 1988) studies of the protein.

lapping the Gly-87 intraresidue cross-peak, however, was observed in the spectrum at pH 7.0 and 40 °C and could be tentatively assigned to the  $d_{\alpha\beta}(i, i + 1)$  peak. [Note that Pro-40 is located in  $\alpha$ -helix 2 and that the  $d_{\alpha\beta}(i, i + 1)$  NOE, like the corresponding  $d_{\alpha\text{N}}(i, i + 1)$  for other amino acids, is expected to be weak in  $\alpha$ -helices.] This, together with the absence of the characteristic  $d_{\alpha\beta}(i, i + 1)$  cross-peak denoting a cis peptide bond, confirms the hypothesis of the presence of a trans 39–40 peptide bond.

A more detailed comparison of the structures of human and *E. coli* thioredoxin than that described here will have to await completion of the determination of the tertiary structure of human thioredoxin. Note, however, that the crystal structure of *E. coli* thioredoxin is of the oxidized form of the enzyme, while this study has focused on the reduced state. No crystal structure of the reduced *E. coli* thioredoxin has been solved as yet (Holmgren, 1985). Detailed comparisons of the two structures should be carried out on molecules in the same oxidation state, since conformational changes accompany a change in oxidation state. Observations, however, regarding the structures of portions of the enzymes removed from the active site may be relevant, as the predominant changes in chemical shift between oxidized and reduced *E. coli* thioredoxin are seen only for those residues immediately adjacent to and within the active site (Hiraoki et al., 1988; Dyson et al., 1988).

*The Two Species of Recombinant Human Thioredoxin.* A comparison of the pattern of the NOEs and apparent  $^3J_{\text{HN}\alpha}$  coupling constants for the two species of recombinant human thioredoxin, one containing and the other lacking the N-terminal methionine, reveals no significant differences (Figure 5) and strongly suggests that the conformations of the two proteins are very similar. The widespread duplication of resonances for 29 different residues that are NOEs primarily at the N- (residues 3–5) and C-termini (residues 101–103), in  $\alpha$ -helix 2 (residues 39 and 41–49), and in  $\beta$ -strands 2 (residues 24–25) and 3 (residues 50–59) may be the result of proximity of the N-terminus to these regions of the molecule. Although the resonances of Met-1 have not been identified, there are NOEs from the  $\text{C}_\beta\text{H}$  and  $\text{C}_\gamma\text{H}_3$  protons of Val-2 to the  $\text{C}_\alpha\text{H}$  proton of His-43, indicating that the N-terminus is in close proximity to  $\alpha$ -helix 2 (residues 35–49). In addition,  $\beta$ -strand 1 (residues 2–5) forms a parallel  $\beta$ -sheet with  $\beta$ -strand 3 (residue 51–58), which in turn forms a parallel  $\beta$ -sheet with  $\beta$ -strand 2 (residues 22–29) as the interstrand NOEs illustrated in Figure 6 make clear.  $\alpha$ -Helix 2 is also in close proximity to  $\beta$ -strands 2 and 3, as well as the C-terminus. This is evidenced by NOEs from the  $\text{C}_\beta\text{H}$  proton of His-43 to a methyl group of Val-25 in  $\beta$ -strand 2, from the aromatic ring of

Phe-42 to main-chain and side-chain protons of Phe-54 and to the NH protons of Leu-55 and Glu-56 in  $\beta$ -strand 3, and from the NH proton of Leu-45 and the  $\text{C}_\alpha\text{H}$  and  $\text{C}_\beta\text{H}$  protons of Tyr-49 to the side chain of Ile-101 at the C-terminus. The above analysis of NOEs in these regions suggest that the primary effects on the chemical shifts of the 29 residues mentioned arise from minor structural perturbations due to the close spatial proximity of the N-terminus to  $\beta$ -strand 3 and  $\alpha$ -helix 2 and that further secondary effects occur as a result of the proximity of these two structural elements to  $\beta$ -strand 2 and the C-terminus. A more detailed interpretation will have to await the determination of the complete three-dimensional structure of human thioredoxin.

#### CONCLUDING REMARKS

The assignment of the  $^1\text{H}$  NMR spectrum and the determination of the secondary structure of the reduced form of human thioredoxin have been presented. Duplicate peaks in the spectra have been shown to arise from the presence of two native forms of the recombinant protein, one containing and the other lacking the N-terminal methionine. The added spectral complexity due to these additional peaks necessitated the use of two sets of temperature and two sets of pH conditions to complete the assignment, and was greatly aided by the increased sensitivity and resolution afforded at 600 MHz. The secondary structure of the protein was determined on the basis of a qualitative interpretation of NOE patterns, amide exchange data, and coupling constant information and was shown to be identical for the two species. The secondary structure homology with the crystal structure of *E. coli* thioredoxin is high, despite moderate amino acid sequence homology.

Studies of the regulation of human thioredoxin synthesis indicate that the enzyme is highly expressed in a number of immunocompetent cells, including established dividing cell lines, such as the lymphoblastoid B cell line from which it was isolated, as well as activated lymphocytes and monocytes. This suggests that human thioredoxin, in addition to functioning in general disulfide chemistry in the cell, may have an important immunological role. A better understanding of all aspects of this protein's function will be considerably aided by the structural studies that are currently being undertaken in our laboratory, leading to the determination of the complete three-dimensional structure of human thioredoxin in solution.

#### ACKNOWLEDGMENTS

We thank Dr. Ad Bax for useful discussions and Dr. Lewis Kay for a critical reading of the manuscript.

#### REFERENCES

- Bax, A. (1989) *Methods Enzymol.* 176 151–168.
- Bax, A., Sklenar, V., Clore, G. M., & Gronenborn, A. M. (1987) *J. Am. Chem. Soc.* 109, 6511–6513.
- Bodenhausen, G., Vold, R. L., & Vold, R. R. (1980) *J. Magn. Reson.* 37, 93–106.
- Braunschweiler, L., & Ernst, R. R. (1983) *J. Magn. Reson.* 53, 521–528.
- Bystrov, V. F. (1976) *Prog. NMR Spectrosc.* 10, 41–82.
- Chang, C. T., Wu, C.-S. C., & Yang, J. T. (1978) *Anal. Biochem.* 91, 13–31.
- Clore, G. M., & Gronenborn, A. M. (1987) *Protein Eng.* 1, 275–288.
- Davis, D. G., & Bax, A. (1985) *J. Am. Chem. Soc.* 107, 2820–2821.
- Driscoll, P. C., Clore, G. M., Ber ss, L., & Gronenborn, A. M. (1989) *Biochemistry* 28, 2178–2187.

- Dyson, H. J., Holmgren, A., & Wright, P. E. (1988) *FEBS Lett.* 228, 254-258.
- Eklund, H., Cambillau, C., Sjöberg, D. M., Holmgren, A., Hoog, J.-O., & Brandén, C.-I. (1984) *EMBO J.* 3, 1443-1449.
- Ernst, R. R., Bodenhausen, G., & Wokaun, A. (1987) *Principles of Nuclear Magnetic Resonance in One and Two Dimensions*, Clarendon Press, Oxford, U.K.
- Hiraoki, T., Brown, S. B., Stevenson, K. J., & Vogel, H. J. (1988) *Biochemistry* 27, 5000-5008.
- Holmgren, A. (1985) *Annu. Rev. Biochem.* 54, 237-271.
- Jeener, J., Meier, B. H., Bachmann, P., & Ernst, R. R. (1979) *J. Chem. Phys.* 71, 4546-4553.
- Kelley, R. F., & Stellwagon, E. (1984) *Biochemistry* 23, 5095-5102.
- LeMaster, D. M., & Richards, F. M. (1988) *Biochemistry* 27, 142-150.
- Macura, C., Huang, Y., Suter, D., & Ernst, R. R. (1981) *J. Magn. Reson.* 43, 259-281.
- Marion, D., & Wüthrich, K. (1983) *Biochem. Biophys. Res. Commun.* 113, 967-974.
- Marion, D., & Bax, A. (1988a) *J. Magn. Reson.* 80, 528-533.
- Marion, D., & Bax, A. (1988b) *J. Magn. Reson.* 79, 352-356.
- Mueller, L. (1987) *J. Magn. Reson.* 72, 191-196.
- Neuhaus, D., Wagner, G., Vasák, M., Kägi, J. H. R., & Wüthrich, K. (1985) *Eur. J. Biochem.* 151, 257-273.
- Pardi, A., Billeter, M., & Wüthrich, K. (1984) *J. Mol. Biol.* 180, 741-751.
- Piantini, U., Sørensen, O. W., & Ernst, R. R. (1982) *J. Am. Chem. Soc.* 104, 6800-6801.
- Plateau, P., & Guéron, M. (1982) *J. Am. Chem. Soc.* 104, 7310-7311.
- Rance, M., Sørensen, O. W., Bodenhausen, G., Wagner, G., Ernst, R. R., & Wüthrich, K. (1983) *Biochem. Biophys. Res. Commun.* 117, 479-485.
- Redfield, A. G., & Kunz, S. D. (1975) *J. Magn. Reson.* 19, 250-254.
- Reutimann, H., Luisi, P.-L., & Holmgren, A. (1983) *Biopolymers* 22, 107-111.
- Söderberg, B.-O., Sjöberg, B.-M., Sonnerstam, V., & Brändén, C.-I. (1978) *Proc. Natl. Acad. Sci. U.S.A.* 75, 5827-5830.
- Thomas, R. M., Boos, R., & Luisi, P.-L. (1986) Folding of Fragments of Thioredoxin from *Escherichia coli*, in *Thioredoxin and Glutaredoxin Systems: Structure and Function*, A. (Holmgren, A., et al., Eds.) pp 87-92, Raven Press, New York.
- Wollman, E. E., d'Auriol, L., Rimsky, L., Shaw, A., Jacquot, J.-P., Wingfield, P., Graber, P., Dessarps, F., Robin, P., Galibert, F., Bertoglio, J., & Fradelizi, D. (1988) *J. Biol. Chem.* 263, 15506-15512.
- Wüthrich, K. (1986) *NMR of Proteins and Nucleic Acids*, Wiley, New York.
- Wüthrich, K., & Wagner, G. (1979) *J. Mol. Biol.* 130, 1-18.
- Wüthrich, K., Billeter, M., & Braun, W. (1984) *J. Mol. Biol.* 180, 715-740.

## Conformation and Reactivity Changes Induced by *N*-Methylkirromycin (Aurodox) in Elongation Factor Tu

C. Balestrieri, A. Giovane, L. Quagliuolo, and L. Servillo\*

Department of Biochemistry and Biophysics, University of Naples, Via Costantinopoli 16, 80138 Napoli, Italy

G. Chinali

Institute of Biological Structures, 2nd Medical School, University of Naples, Via Pansini 5, 80100 Napoli, Italy

Received November 3, 1988; Revised Manuscript Received February 21, 1989

**ABSTRACT:** Kirromycin and related antibiotics inhibit protein synthesis in bacteria by acting on elongation factor Tu (EF-Tu). We have studied the effects of *N*-methylkirromycin (aurodox) on some molecular properties of this protein. The binding of the antibiotic causes a dramatic variation in the protein fluorescence emission spectrum with the appearance of a new maximum at around 340 nm. Addition of aurodox to trypsinized EF-Tu resulted in an emission spectrum similar to that of the denatured intact factor. Fluorescence lifetime analysis performed by a multifrequency phase fluorometer indicated that the fluorescence emission of the factor is heterogeneous with the major component having a lifetime near 4.8 ns in the absence and 6.6 ns in the presence of the antibiotic. These results were interpreted in terms of an antibiotic-induced environmental modification of the unique tryptophan residue of the protein leading to an increase in its quantum yield. However, aurodox did not modify the solvent exposure of this residue, as judged by fluorescence quenching experiments. Moreover, 1-anilino-8-naphthalenesulfonate (ANS) binding studies, as well as analysis of the protein reactivity toward the sulfhydryl group reagent 5,5'-dithiobis(2-nitrobenzoate) (DTNB), showed that, in the presence of aurodox, the behavior of the EF-Tu-GDP complex nears that of EF-Tu-GTP. These results strongly support the hypothesis that aurodox not only confers a "GTP-like" conformation to the EF-Tu-GDP complex but also produces a less stable folding of the protein around the tryptophan residue that may contribute to the multiple functional effects of this antibiotic.

The first step of each elongation cycle in protein biosynthesis is promoted by elongation factor Tu (EF-Tu)<sup>1</sup> which forms

a ternary complex, with GTP and aa-tRNA, that binds to mRNA-programmed ribosomes. As a result, GTP is hydro-